



# Future changes in the wintertime cyclonic activity over the CORDEX-CORE southern hemisphere domains in a multi-model approach

Michelle Simões Reboita<sup>1,2</sup> · Marco Reale<sup>2,3</sup> · Rosmeri P. da Rocha<sup>4</sup> · Filippo Giorgi<sup>2</sup> · Graziano Giuliani<sup>2</sup> · Erika Coppola<sup>2</sup> · Rosa Beatriz Luna Nino<sup>5</sup> · Marta Llopart<sup>6,7</sup> · Jose Abraham Torres<sup>2</sup> · Tereza Cavazos<sup>5</sup>

Received: 28 December 2019 / Accepted: 26 May 2020 / Published online: 2 June 2020  
© Springer-Verlag GmbH Germany, part of Springer Nature 2020

## Abstract

Changes in the characteristics of austral winter (June–July–August) synoptic activity in three domains (Africa, Australia and South America) of the extratropical Southern Hemisphere projected with the Regional Climate Model version 4 (RegCM4) are presented. The model is nested in three global climate models (GCMs) from the Coupled Model Intercomparison Project phase 5 (CMIP5) under the Representative Concentration Pathway 8.5. The model grid spacing is 25 km and the simulations cover the period 1970–2100. Synoptic activity is analyzed using both Eulerian and Lagrangian approaches. The Eulerian analysis shows an increase of the synoptic activity south of 40° S in the RegCM4 and GCMs ensembles for the future (2080–2099) compared to the present (1995–2014), but this signal does not necessarily indicate an increase in the cyclone frequency since it includes cyclonic and anticyclonic features. The Lagrangian analysis, however, indicates a decrease in the frequency of cyclones, with a positive tendency towards stronger systems, although the latter is not statistically significant at 95% confidence level. Lifetime, traveled distance and mean speed of the cyclones do not present statistically significant changes in the future climate. On the other hand, a significant increase in both intensity and extension of areas affected by precipitation associated with cyclones is found. As a consequence, there is a statistically significant trend of individual cyclones to produce more rainfall in the future.

**Keywords** Extratropical southern hemisphere · Cyclones · Precipitation · Cyclone tracking scheme · RegCM4 · CORDEX-CORE

## 1 Introduction

Cyclones out of the tropics, which are the focus of this study, are responsible for abrupt changes of local weather conditions, in terms of precipitation (e.g. Catto et al. 2015) and winds (e.g. Ashley and Black 2008; Bitencourt et al. 2011). Strong winds produced by extratropical and subtropical cyclones can disrupt the aero and maritime transport, interrupt power supplies and cause storm surges affecting coastal regions etc. (da Rocha et al. 2004; Nissen et al. 2010; Pepler et al. 2016; Brasiliense et al. 2018; Lionello et al. 2019; Reboita et al. 2019a). Cyclones are the main cause of precipitation at mid-latitudes (Hawcroft et al. 2012; Huntingford et al. 2014; Reboita et al. 2018; Kodama et al. 2019), and flooding in coastal regions (Pitt 2008; Pfahl and Wernli 2012; Hawcroft et al. 2018; Lionello et al. 2019). In addition, extratropical cyclones are extremely important for the climate system, since they redistribute heat and moisture

✉ Michelle Simões Reboita  
reboita@unifei.edu.br

- <sup>1</sup> Federal University of Itajubá, UNIFEI, Itajubá, MG, Brazil
- <sup>2</sup> Earth System Physics, ESP, The Abdus Salam International Centre for Theoretical Physics, Trieste, Italy
- <sup>3</sup> Istituto Nazionale di Oceanografia e Geofisica Sperimentale OGS, 34151 Trieste, Italy
- <sup>4</sup> Departamento de Ciências Atmosféricas, Universidade de São Paulo, USP, São Paulo, Brazil
- <sup>5</sup> Department of Physical Oceanography, Ensenada Center for Scientific Research and Higher Education, CICESE, Ensenada, Mexico
- <sup>6</sup> Universidade Estadual Paulista, UNESP, Bauru, SP, Brazil
- <sup>7</sup> Centro de Meteorologia de Bauru, IPMet, Bauru, SP, Brazil

between mid-latitude and polar regions (Peixoto and Oort 1992; Fasullo and Trenberth 2008; Shaw et al. 2016).

In extratropical regions, the main climatological features of cyclones can be obtained through Eulerian and Lagrangian methods. The former was introduced by Blackmon (1976), and is based on the analysis of the variance of the synoptic time-scale bandpass-filtered Sea Level Pressure (SLP) fields. Since then, this method has been applied in several studies (e.g., Hoskins and Hodges 2019). The Lagrangian method is based on the detection and tracking of individual storms using automatic procedures applied to the SLP, relative vorticity or other appropriate meteorological fields (Murray and Simmonds 1991; Sinclair 1994; Lionello et al. 2002; Hoskins and Hodges 2005; Lionello and Giorgi 2007; Ulbrich et al. 2009, 2013; Neu et al. 2013; Reale et al. 2013; Reboita et al. 2015, 2018; Lionello et al. 2016; Flaounas et al. 2018; Reale et al. 2019; Kodama et al. 2019). One of the first studies using an algorithm to track extratropical cyclones was developed by Murray and Simmonds (1991).

Both approaches are widely used not only on reanalysis data (e.g. Neu et al. 2013; Reboita et al. 2015) but also on General Circulation Model (GCMs, e.g. Ulbrich et al. 2013) and Regional Climate Models data (RCMs, e.g. Lionello and Giorgi 2007; Reboita et al. 2010, 2018; Flaounas et al. 2018). Some modeling studies have investigated the behavior of cyclones in future climate in several regions of the world. For example, Yin (2005), Bengtsson et al. (2009), and Grieger et al. (2014) analyzed GCMs projections and found a poleward shift of the storm tracks and, in conjunction with it, a predominant decrease in the frequency of cyclones in the Southern Hemisphere (Chang et al. 2016), especially the strongest (Michaelis et al. 2017).

Lionello and Giorgi (2007) employed for the first time an RCM to evaluate climate change impacts on the cyclone climatology for the Mediterranean region. They used the Regional Climate Model version 3 (RegCM3; Pal et al. 2007), under the A2 and B2 scenarios of the Intergovernmental Panel on Climate Change (IPCC), and found an increase (decrease) in the winter cyclonic activity over western Europe (in the Mediterranean area), an intensification of cyclones in the north Mediterranean and a northward shift of the mid-latitude storm tracks. Reboita et al. (2010) were the first to simulate the climatology of extratropical cyclones over the South Atlantic Ocean with a RCM, in this case also the RegCM3. The model was able to reproduce the main features of the cyclone activity in the three cyclogenetic regions near the South America coast (southeastern Brazil, south Brazil/Uruguay and southeastern Argentina). Similarly, Krüger et al. (2012) nested RegCM3 in the HadAM3 GCM for downscaling the cyclone climatology over the South Atlantic Ocean and found a decrease in the total number of cyclones of  $-7.2\%$  and  $-4.7\%$  for the A2 and B2 scenarios,

respectively. Recently, Reboita et al. (2018) nested the RegCM4 model (Giorgi et al. 2012) in the HadGEM2-ES GCM under the RCP8.5 scenario (Moss et al. 2010) over the South Atlantic Ocean. For the end of the century, they found a decrease up to  $-6.5\%$  in the annual frequency of cyclones in RegCM4 and  $-3.6\%$  in HadGEM2-ES, in agreement with the estimations provided by Krüger et al. (2012). Similar to these authors, the projections of Reboita et al. (2018) did not indicate any statistically significant future change in the mean intensity of the cyclones.

Considering Australia and the oceans surrounding this continent, Bengtsson et al. (2006) found an end-of-century (2070–2100) decrease of cyclone activity around  $40^\circ$  S over southern Australia and part of New Zealand with the ECHAM5-OM1 GCM under the A1B scenario. Other studies on subtropical and extratropical cyclones have focused mainly on the eastern sector of Australia. For example, Dowdy et al. (2013), using the HadCM3.0 GCM under the A2 scenario, found that the frequency of cyclones associated with heavy precipitation events in this region is projected to decrease by 8–25% by the end of the twenty-first century, depending on season and latitude. Pepler et al. (2016) carried out the first projections of future cyclone activity near the eastern coast of Australia using a RCM ensemble and obtained a decrease in the cyclone's frequency during the austral winter. However, in contrast to Dowdy et al. (2013), they found a potential increase in the frequency of cyclones associated with heavy rainfall in the future.

Specific studies regarding climate projections of cyclones over southern Africa and adjacent oceans are scarce. Some information can be extracted from studies focusing on the whole Southern Hemisphere. Geng and Sugi (2003) showed that the frequency of extratropical cyclones is projected to decrease by approximately 10% by 2050, but intense cyclones become more frequent, mainly over the southeastern coast of South Africa and South America. Using a multi-model ensemble of GCMs under the A1B scenario, Grieger et al. (2014) also found a decrease in the frequency of cyclones northward of  $50^\circ$  S. From the analysis of 26 GCMs projections, southern Africa may be affected by dry conditions during winter in the mid-century (2040–2060), possibly due to the decrease in the frequency of cold fronts associated with extratropical cyclones (Mahlalela et al. 2019). In addition, changes in the location of the storm tracks may have severe consequences for the water supply of several regions, including southern Africa (Bengtsson et al. 2006).

According to the studies previously mentioned and the IPCC-AR5 (2013), a poleward storm track displacement is mostly expected in the future climate, along with a decrease of extratropical cyclones frequency at mid-latitudes. However, there are large uncertainties related to the projected change in the intensity of the cyclones (Ulbrich et al. 2009;

Bader et al. 2011; Feser et al. 2015). Even so, some studies for the Southern Hemisphere point in the same direction, e.g. Chang (2017) found a significant increase in the frequency of extreme cyclones (using different definitions of extreme) in all seasons based on 26 CMIP5 GCMs under the RCP8.5 scenario. Similarly, using reanalysis data, Reboita et al. (2015) obtained an increase in the frequency of intense cyclones and a decrease in the frequency of weak systems over the Southern Hemisphere during the last decades. These trends are consistent with the slight increase in the number of intense cyclones in the future climate simulations for Southern Hemisphere winter found by Kodama et al. (2019) and Grieger et al. (2014). This late study focused on an ensemble of nine coupled AOGCM integrations from six different models and showed an increase in the number of strong cyclone tracks, but only three AOGCMs showed statistically significant increases ( $p < 0.05$ ).

The increase of greenhouse gas concentration in the atmosphere produces amplified warming at high latitudes (Lu and Cai 2009; Francis and Varus 2012). As a consequence, there is a reduction of the meridional equator-pole temperature gradient in the lower troposphere, implying less available potential energy for extratropical cyclones. On the other hand, in a warmer scenario, the evaporation increases, contributing to enhancing tropical convection and warming at the tropical upper-troposphere. This further strengthens the baroclinicity at upper levels (upper-level jets), which enhances synoptic activity at the surface (Mizuta et al. 2011). Because of the increased convection, warming of the upper troposphere is expanded polewards (Reichler 2009 presents a review of observational studies that documented this expansion), leading to the poleward displacement of the upper-level jets and storm tracks. Studies by Yin (2005), Kodama and Iwasaki (2009), Rivière et al. (2012), and Reboita et al. (2018) have indeed found a poleward displacement of the upper-level jets in scenarios of climate change, along with a poleward displacement of the Hadley cell and subtropical anticyclones (see Reboita et al. 2019b; and references therein).

In warming scenarios, the increase of atmospheric water vapor (Booth et al. 2013) can contribute to increasing the precipitation associated with cyclones (Bengtsson et al. 2009; Zappa et al. 2013; Hawcroft et al. 2018; Kodama et al. 2019). For example, Blazquez and Solman (2018) found an increase in the precipitation associated with fronts and cyclones over the Southern Hemisphere under the RCP4.5 in winter. On the other hand, Reboita et al. (2018) identified a decrease of ~15% of precipitation in mid-latitudes over the central portion of the South Atlantic Ocean under RCP8.5 in terms of annual mean. Michaelis et al. (2017) also suggest that the increase of the atmospheric water vapor in scenarios of climate change could result in a more efficient poleward heat transport by extratropical cyclones, resulting

in a decrease of the number or strength of eddies responsible to move energy polewards.

It is clear from this brief review that, although some consistent signals on extratropical cyclone changes are emerging, such as a reduced frequency of cyclones, still large uncertainties are present. For example, climate change studies do not show conclusive results on the intensity of these systems. Besides, results may be strongly region-dependent, so that a cross-regional analysis is needed. Finally, it has been pointed out that high resolution may be needed to properly resolve the structure of cyclones (e.g. Michaelis et al. 2017), for which RCMs are an optimal resource.

All these issues can be addressed taking advantage of a recent initiative called CORDEX-CORE (Coordinated Regional Downscaling Experiment (CORDEX)-Coordinated Output for Regional Evaluations (CORE); Gutowski et al. 2016) under which a new ensemble of RCM-based projections was completed for a number of domains defined by the CORDEX program (Giorgi et al. 2009). Using this newly available dataset, in this study we analyze the projected changes in cyclone (out of the tropics) characteristics (location, frequency, depth, lifetime, traveled distance, mean speed, and precipitation) during the austral winter (JJA), when cyclogenesis is more frequent. We focus on three domains in the Southern Hemisphere, i.e. South America, Africa and Australia, following a multi-model ensemble approach. Data are analyzed from simulations completed with the RegCM4 RCM at 25 km grid spacing driven by three GCMs (Hadley Center Global Environment Model version 2, Max Planck Institute Earth System Model and Norwegian Earth System Model) under the RCP8.5 scenario. Some details about experiment set up are provided in Sect. 2; results are discussed in Sect. 3 while conclusions are in Sect. 4.

## 2 Methodology

### 2.1 Global climate models

Three GCMs from CMIP5 provided initial and lateral boundary conditions for the RegCM4 simulations: the Hadley Center Global Environment Model version 2 (HAdGEM2-ES, Collins et al. 2008), the Max Planck Institute Earth System Model (MPI-ESM-MR, Giorgetta et al. 2013), and the Norwegian Earth System Model (NorESM-1M; Bentsen et al. 2012). Table 1 shows the horizontal and vertical resolution of these GCMs. They were chosen as base driving models in the CORDEX-CORE effort because of their relatively good performance in reproducing present-day climate over different domains (Elguindi et al. 2014) and because they roughly cover the CMIP5 range of climate sensitivity

**Table 1** Horizontal and vertical grids of the three GCMs and access links

GCM	Horizontal grid spacing (in degrees)	Number of vertical levels	Access links
HadGEM2-ES	1.25 × 1.875	60	<a href="https://portal.enes.org/models/earthsystem-models/metoffice-hadley-centre/hadgem2-es">https://portal.enes.org/models/earthsystem-models/metoffice-hadley-centre/hadgem2-es</a>
MPI-ESM-MR	1.875 × 1.875	95	<a href="https://www.mpimet.mpg.de/en/science/models/mpiesm/">https://www.mpimet.mpg.de/en/science/models/mpiesm/</a>
NorESM-1 M	1.90 × 2.50	26	<a href="https://portal.enes.org/models/earthsystem-models/ncc/noresm">https://portal.enes.org/models/earthsystem-models/ncc/noresm</a>

(HadGEM2-ES, MPI-ESM-MR and NorESM-1 M being high, intermediate and low sensitivity models, respectively).

## 2.2 Regional climate model version 4 (RegCM4)

RegCM4 is a regional climate model that solves the atmospheric dynamics in a sigma-pressure vertical coordinate system (Giorgi et al. 2012). The model participates in the CORDEX-CORE program (Gutowski et al. 2016), and has been used in the hydrostatic configuration to complete projections on 9 CORDEX domains (3 for the Southern Hemisphere) at 25 km grid spacing and 23 sigma-pressure levels. Here we focus on the Southern Hemisphere domains (Fig. 1): Africa (AFR), Australia (AUS) and South America (SAM).

The model was customized to optimize its performance based on a series of preliminary experiments that revealed the more appropriate physical configuration for each domain (Sines 2018a, b). Some physics schemes are common to the

AFR, AUS and SAM domains: Holtslag (Holtslag et al. 1990; Holtslag and Boville 1993) for the boundary layer processes, Common Land Model (CLM4.5; Oleson et al. 2013) for land–atmosphere interaction, Kiehl et al. (1996) modified as described in Giorgi et al. (2012) for radiative transfer processes, Zeng et al. (1998) for the representation of turbulent fluxes over the sea (Zeng et al. 1998) and the SUBEX scheme (Pal et al. 2000) for the description of resolvable scale clouds and precipitation. Only the cumulus convection parameterization differs as a function of domain: AFR and SAM used Tiedtke (1989) over the land and Kain-Fritsch (1990) over the ocean, while AUS used the Tiedtke scheme for both land and ocean.

The simulations cover the period 1970–2100, with the scenarios starting in 2006. Following the IPCC recommendation for AR6, we analyze the reference period 1995–2014 (hereafter historical period) and the end-of-century period 2080–2099 (hereafter far-future period). For AFR only two

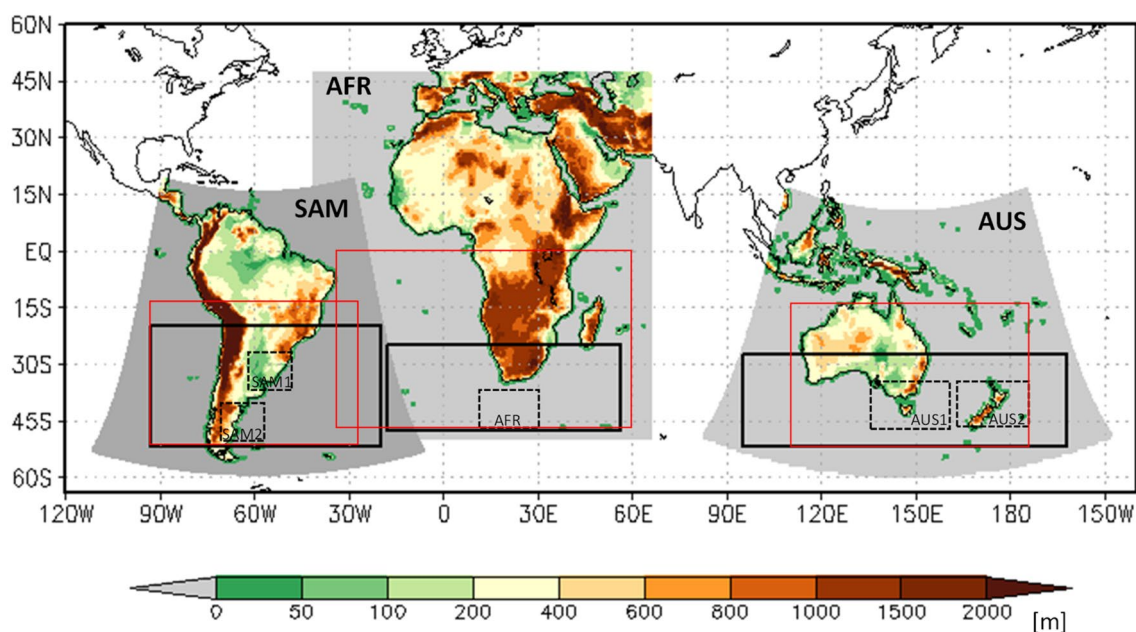


**Fig. 1** Southern Hemisphere CORDEX domains, topography (meters), areas used in the Eulerian analysis (red boxes) and Lagrangian analysis (black boxes), and areas hotspots of cyclogenesis (dot boxes). Domains coordinates are AFR: 10° E–30° E and 45° S–38° S;

AUS1: 145° E–165° E and 46° S–35° S; AUS2: 170° E–190° E and 46° S–35° S; SAM1: 66° W–46° W and 37° S–25° S and SAM2: 70° W–55° W and 50° S–38° S

projections are available: RegCM4 nested in HadGEM2-ES and in NorESM-1M (therefore, for this domain we also considered two projections in the GCM analysis).

## 2.3 Validation data

In order to assess the performance of both the GCMs and RegCM4 ensembles in reproducing the synoptic activity and precipitation distribution in the historical period two datasets are used: SLP fields from the European Centre for Medium-Range Weather Forecasts (ECMWF) Interim reanalysis (hereafter ERAI; Dee et al. 2011) with 6-h intervals and a grid spacing of  $0.75^\circ$ , and gridded daily precipitation data from Global Precipitation Climate Project (GPCP version v1.3, Huffman et al. 2001) with a grid spacing of  $1^\circ$ .

## 2.4 Cyclone identification

SLP is analysed following two approaches (Eulerian and Lagrangian) to define the synoptic activity over the Southern Hemisphere.

### 2.4.1 Eulerian method

The Eulerian method is based on the analysis of the SLP variability using the standard deviation of the 2–6-day bandpass filtered fields (Blackmon 1976). We refer to this variable as “synoptic signal”, which can be used to illustrate the geographic distribution of the storm tracks (Hoskins and Hodges 2005; Lionello and Giorgi 2007; Lionello et al. 2008).

### 2.4.2 Lagrangian method

The Lagrangian method used here is an automatic cyclone detection and tracking method (CDTM) developed by Lionello et al. (2002) and Reale and Lionello (2013), which has been compared with other tracking schemes in the Inter-comparison of Mid Latitude STorm Diagnostics (IMILAST; Neu et al. 2013) project. The CDTM is based on the search of pressure minima in the SLP field at time intervals of 6 h using a nearest neighbor approach. One grid point is considered as cyclone center if the SLP is lower than the SLP of the 8 nearest grid points (Lionello et al. 2002). The trajectory of a system is obtained by joining the location of the low-pressure center in successive SLP fields. The final result of the algorithm is the central position (latitude and longitude), SLP minimum (in hPa), Laplacian (in  $\text{hPa m}^{-2}$ ) and depth (hPa) for each time step of the cyclone lifecycle.

According to Reale and Lionello (2013), the depth of each system is obtained through estimation of the difference between the SLP background field and SLP minimum at the center of the cyclone. Therefore, depth can be used

as a measure of the cyclone intensity. From the geographical coordinate of the cyclones, it is possible to compute the cyclone density defined as the ratio between the number of cyclones in a region and the area of this region itself. In this study, the area is defined as a  $3^\circ \times 3^\circ$  latitude–longitude box and the density is calculated only considering the first position of the cyclones (cyclogenesis).

Cyclones were tracked in both GCMs and RegCM4 SLP projected fields and in ERAI. Before applying the CDTM, each individual field from GCMs and RegCM4 was interpolated on a regular grid of  $0.75^\circ \times 0.75^\circ$ , which is the same grid spacing as ERAI, and considering the same subdomains shown in Fig. 1 (AFR, AUS and SAM). The cyclone climatologies include only systems with lifetime equal or higher than 24 h reaching a depth equal or higher than 10 hPa in some period of their lifecycle. The depth threshold of 10 hPa was chosen to exclude weak systems (Lionello et al. 2002). GCMs and RegCM4 ensemble averages were computed after performing the calculations for each projection separately.

## 2.5 Analysis

The first part of the results shows the Eulerian analysis while the second presents the main climatological features of the cyclones (frequency, density, lifetime etc.) obtained from the Lagrangian CDTM tracking. The last part of the study focuses on the precipitation associated with cyclones. Following Reboita et al. (2012), for each domain, hotspot cyclogenetic regions are selected (Fig. 1) and the average precipitation associated with cyclones in that region is calculated over a three-day period (pre-cyclogenesis, cyclogenesis and post-cyclogenesis). The climate change signals are calculated as the difference of future minus present statistics based on the time slices mentioned above and the RegCM4 and GCMs ensembles.

## 3 Results

### 3.1 Eulerian approach

Figure 2a–c show the bandpass filtered synoptic-scale standard deviation (2–6 days) of SLP in ERAI, and the GCMs and RegCM4 ensembles. In all domains, the standard deviation is higher south of  $40^\circ$  S, with the largest values over the AFR domain. There is also considerable synoptic-scale activity from  $25^\circ$  to  $40^\circ$  S over South America. These results are in agreement with previous studies (e.g. Hoskins and Hodges 2005). The standard deviation biases have a similar spatial pattern in the RegCM4 and GCMs ensembles, with an underestimation of synoptic-scale variability over most of the South Atlantic Ocean and AFR domain (Fig. 2d, e). The biases are in general smaller over the AUS domain.

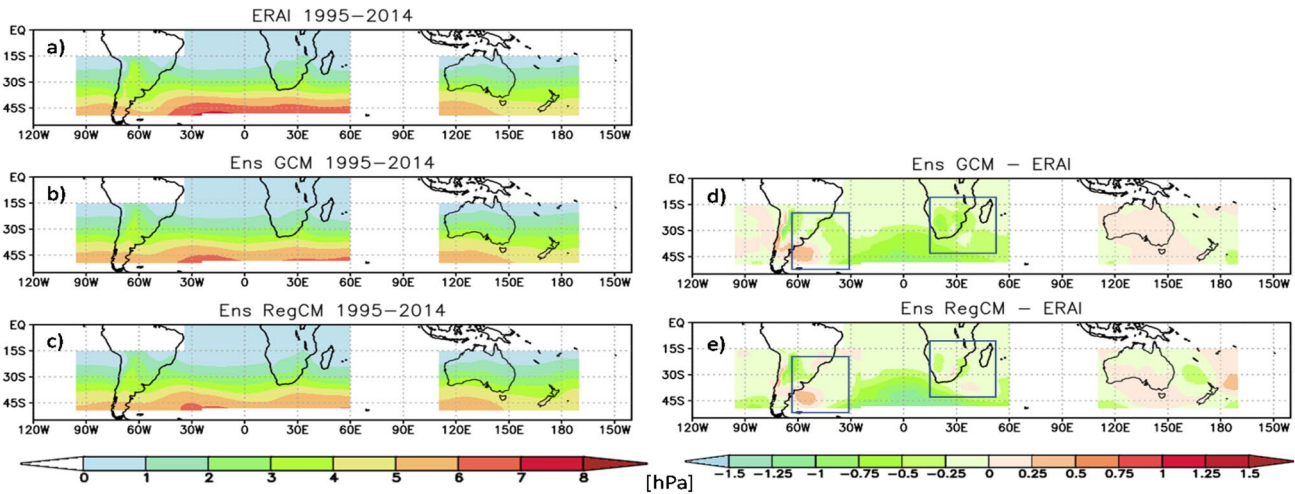


**Fig. 2** Bandpass-filtered (2–6 day) variance converted to the standard deviation for SLP during austral winter in the historical period (1995–2014): **a** ERAI, **b** GCMs ensemble, **c** RegCM4 ensemble, **d** difference GCMs-ensemble minus ERAI, and **e** RegCM4-ensem-

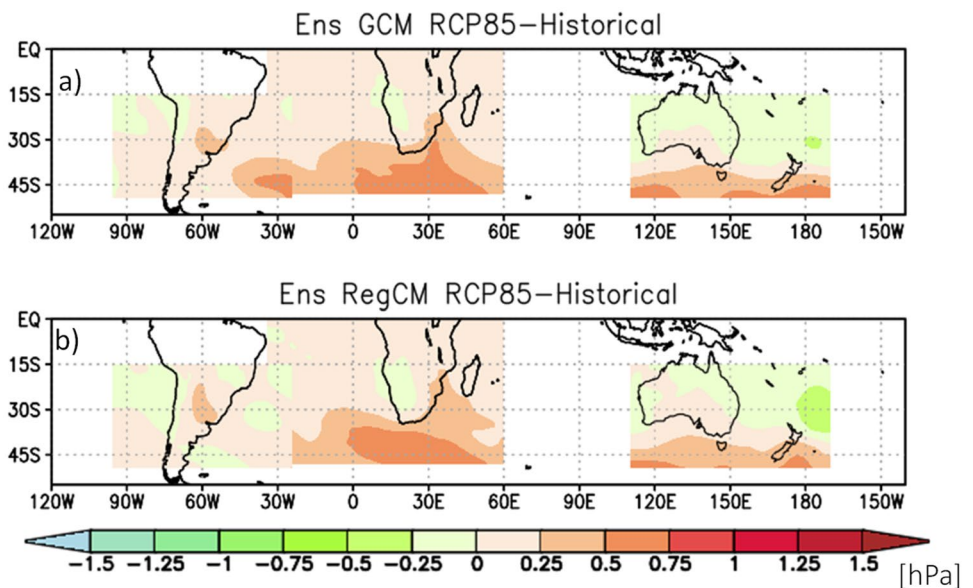
ble minus ERAI. In **d** and **e** the black box indicates the areas that RegCM4-ensemble has lower differences in relation to ERAI than the GCMs-ensemble

Figure 2d, e also shows that, compared with the GCMs, the RegCM4 ensemble improves the representation of synoptic-scale variability mostly from southern Africa to the Indian Ocean, southeastern South America and western South Atlantic. In these latter two regions, the improvement can be associated with a more realistic representation of synoptic systems developing downstream of the Andes Mountains. The RegCM4 topography may also account for the smaller biases over continental Africa and downstream over the Indian Ocean. These RegCM4 improvements, however, are not found over the southern sector of

the South Atlantic (from 30° W to 20° E) where the GCM ensemble has smaller biases.

Projections for the RCP8.5 climate change scenario are shown in Fig. 3. The main difference between RegCM4 and GCMs is the stronger positive trend in the GCMs ensemble for the SAM domain. Considering both ensembles, an increase of synoptic-scale activity occurs mainly over the oceans south of 40° S. Over the continent, there is an increase of synoptic-scale activity over the Uruguay-south Brazil region and east of South Africa in both the RegCM4 and GCMs ensembles, this increase being slightly higher in the GCMs than the RegCM4.

**Fig. 3** Difference future (2080–2099) minus historical (1995–2014) period of the bandpass-filtered (2–6 day) standard deviation for SLP



The increase in synoptic activity for the future climate does not necessarily indicate an increase in cyclone frequency, since the Eulerian variance is a diagnostic of both cyclonic and anticyclonic synoptic systems. Past literature has highlighted an increase in mid-latitude anticyclonic activity. For example, Pepler et al. (2018) found an increase in the frequency of anticyclones southward 30° S over the Southern Hemisphere in reanalysis data. Moreover, Reboita et al. (2019b) obtained a positive trend of SLP southward 30° S in different CMIP5-GCMs under the RCP8.5 scenario, and this signal was also found in CMIP3-GCMs over SAM (Seth et al. 2010; Krüger et al. 2012). These studies suggest a future decrease of cyclone frequency and/or intensity and/or an intensification of the anticyclone features (frequency and/or intensity) at mid-latitudes.

As the Eulerian approach does not allow separating cyclones from anticyclones, the Lagrangian method is a better tool to identify separately these systems (Hoskins and Hodges 2005) and to make clear what synoptic systems determine the higher variance provided by the Eulerian analysis. Here, however, we apply the Lagrangian analysis only to the study of cyclones. The analysis of anticyclones in the climate scenarios over the Southern Hemisphere is beyond the scope of the present work and will be explored in a future study.

### 3.2 Lagrangian approach

#### 3.2.1 Cyclogenesis density

Figure 4 presents the cyclogenesis density obtained with the Lagrangian method for the present climate. According to ERAI, the main feature for the SAM domain consists of two cores of higher cyclogenesis density at the eastern coast of South America (southern Brazil-Uruguay and southeastern Argentina; Fig. 4a). These cores are in agreement with previous winter climatologies calculated by Gan and Rao (1991), Hoskins and Hodges (2005) and Reboita et al. (2010, 2015, 2018). Dynamically, the maximum over the southern Brazil-Uruguay region (~30° S) is mainly associated with baroclinic waves traveling at mid-levels from the Pacific to the Atlantic Ocean. The core in southeastern Argentina (~45° S) results from near-surface horizontal temperature gradients and from cyclones that regenerate after crossing the Andes Mountains. Another cyclogenetic density core is centered in ~45° S-40° W, over the South Atlantic Ocean, east of the continent as in Reboita et al. (2010, 2018). Over the Pacific Ocean, the maximum activity of cyclogenesis is found near 45° S-90° W.

In the SAM domain, the spatial pattern and intensity of cyclogenesis density simulated by RegCM4 are more similar to the ERAI than those simulated by the GCMs (Fig. 4a-c), which show a general underestimation of cyclogenesis density. One deficiency of both ensembles is the underestimation of cyclones near Uruguay and southern Brazil. In a previous analysis, Reboita et al. (2010) discussed how this depends on (a) mid-level waves with lower amplitude in the

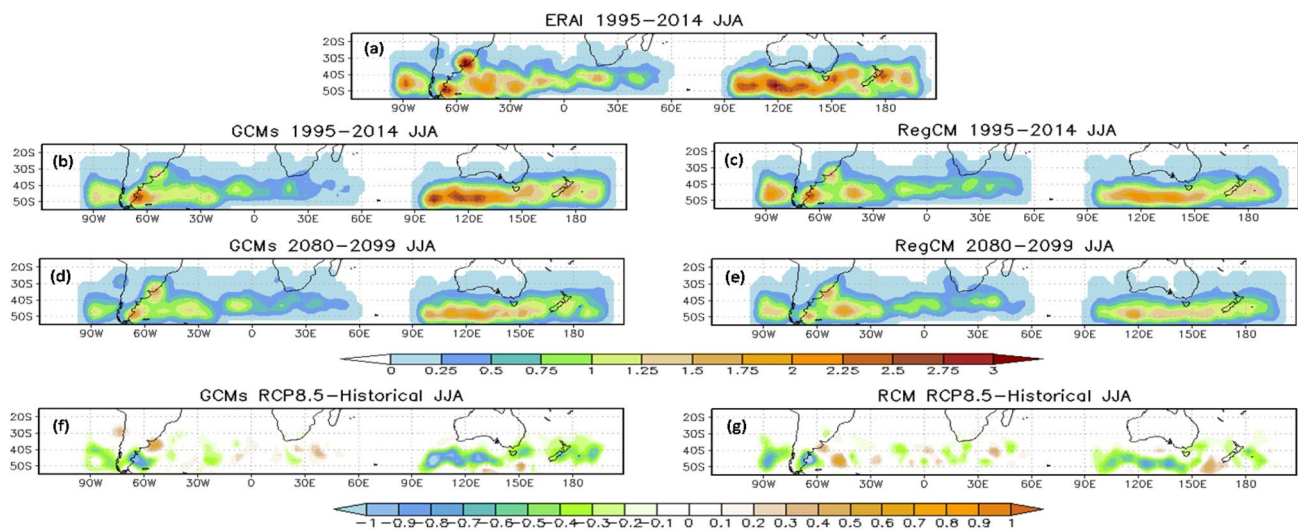


**Fig. 4** Cyclogenesis density [(number of systems in regions of 3°×3°/area of the regions)×10<sup>6</sup>]. **a** ERAI, **b** GCMs ensemble and **c** RegCM4 ensemble in the historical period; **d**, **e** in the RCP8.5 scenario and **f**, **g** the differences future (2080–2099) minus historical

period (1995–2014). A statistical significance test was not included in the projection figures since it tends to be very patchy as a function of high time–space variability of the cyclones (Pezza et al. 2012)

RegCM simulation than reanalysis, and (b) RegCM underestimating the low-level moisture transport from Amazonia to the region. In terms of climate change signal, near the Argentina coast, south of 40° S, both ensembles project a decrease in cyclogenesis density, while the change is positive over the Uruguay coast (Fig. 4f, g). Similar results were found by Reboita et al. (2018) using RegCM4 with a horizontal grid spacing of ~50 km nested in HasGEM2-ES. Possible reasons for the increase of cyclone frequency near Uruguay are the intensification of the subtropical jet at 200 hPa (Reboita et al. 2018) and the low-level moisture input organized by anomalous northeasterly–easterly winds from the southwestern South Atlantic Ocean (Krüger et al. 2012; Nuñez and Blázquez 2014; Llopart et al. 2020).

The GCMs ensemble simulates the intensity of cyclogenesis density closer to ERAI than RegCM4 in the AUS domain (Fig. 4). The maximum cyclogenetic band is located more southward, near 50° S, than in the other domains. There is also a pronounced cyclogenetic activity over southeastern Australia and eastern New Zealand, in agreement with previous studies (Hoskins and Hodges, 2005; Reboita et al. 2015). These two cyclogenetic cores are formed by extratropical and subtropical cyclones (Pepler et al. 2016; Dowdy et al. 2019) related to a range forcing mechanisms (mid-latitude baroclinic drivers, cutoff lows, diabatic heating due convective clouds, release of conditional instability etc.), and with the cyclones being more frequent in winter (Ji et al. 2018). On the other hand, the zonal cyclogenetic bands, in general south of 40° S, in all domains are associated with mid-latitude baroclinicity. For the end of the century, we find a general decrease in the frequency of cyclones over most of the AUS domain (Fig. 4f, g), including southeastern Australia, New Zealand and the downstream regions. The negative trends are higher in the GCMs than the RegCM4 ensemble (Fig. 4f-g). In addition, RegCM4 projects a large area with an increase of cyclonic activity centered near 160° W–50° S, which is much smaller in the GCMs and displaced eastward.

Over the AFR domain, ERAI shows three main cyclogenetic density maxima in the same zonal band, one over the Atlantic Ocean (centered ~45° S–15° E) and two south of

the continent, centered around ~42° S (Fig. 4a). Both the GCMs and RegCM4 ensembles underestimate the cyclogenetic density in the AFR domain, mainly over its eastern sector (southern Madagascar). In this domain, RegCM4 shows an improved spatial representation of the main cyclogenetic cores compared to the GCMs (Fig. 4a–c). Future climate projections indicate areas with weak increases and decreases of cyclogenesis density, with the signals being more intense in RegCM4 (Fig. 4f).

The projected changes in the cyclogenesis density obtained from the Lagrangian approach (Fig. 4f, g) can be linked with the results of the Eulerian analysis (Fig. 3c–e). In general, the same regions with increase in the SPL variance in mid-latitudes (Eulerian analysis) present decrease in the cyclogenesis frequency, which agrees with the positive trend of anticyclones frequency and SPL at those latitudes (Pepler et al. 2018; Reboita et al. 2019b). On the other hand, between 30° and 40° S near Uruguay (SAM domain), greater variance over the continent in the Eulerian analysis is connected with the higher frequency of cyclones displaced to the south in the Lagrangian analysis.

### 3.2.2 Mean features

While Fig. 4 shows the spatial distribution of cyclogenesis density, Table 2 is a summary of the average number of cyclones (systems with depth  $\geq 10$  hPa) found during the austral winter in each domain.

Table 2 shows that in SAM and AFR, RegCM4 has smaller biases than the GCMs in reproducing the observed frequency of cyclones, with the opposite occurring in AUS. The better performance of RegCM4 over SAM and AFR may be associated with two main features: (a) the greater experience in assessing and optimizing the RegCM4 over the SAM (Reboita et al. 2014, 2018; Llopart et al. 2020) and AFR (Mbienda et al. 2016; Ogwang et al. 2016; Koné et al. 2018; Adeniyi 2019) compared to AUS (Song et al. 2008), and (b) the greater influence of topography in the cyclone formation over SAM, which organizes the Rossby wave propagation downstream of the Andes Mountains influencing the cyclogenesis over the east coast of SAM

**Table 2** Mean occurrence of cyclones in JJA over the three Southern Hemisphere domains

Datasets	Domains					
	AFR		AUS		SAM	
	Historical	Future	Historical	Future	Historical	Future
ERAI	7.9	–	26.1	–	17.5	–
GCM	5.0	5.0 (0)	21.8	16.2 (– 5.6)	12.8	11.6 (– 1.2)
RegCM	7.0	6.2 (– 0.8)	16.6	13.3 (– 3.3)	14.8	12.2 (– 2.6)

The difference future minus present is in parentheses. The statistically significant values (considering  $\alpha=0.05$ ) of these differences are in bold while the statistically significant differences of the models in relation to ERAI in the historical period are in italic



and over the ocean (Vera et al. 2002; Reboita et al. 2012; Gramscianinov et al. 2019); such an effect may also occur in the AFR domain. For AUS, we also suggest that the weak performance of the RegCM4 compared to the GCMs may be associated to the domain area, which may not be large enough to represent adequately all cyclogenesis processes.

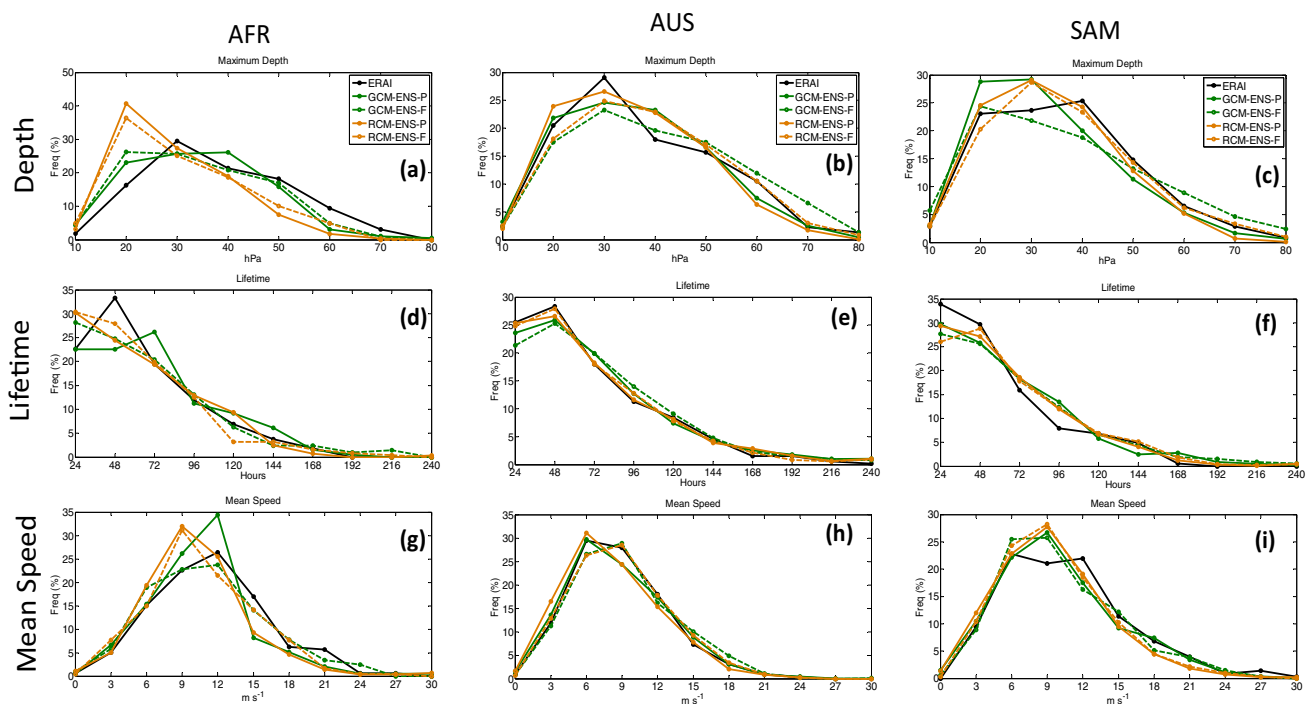
AUS (AFR) is the domain with the highest (lowest) frequency of cyclones in both present and future climate conditions (Table 2). Except for AFR, a statistically significant (95% confidence level) decrease of cyclone frequency is found at the end of the century. For the AUS domain, the GCMs ensemble projects a decrease in cyclone frequency of 5.6% and the RegCM4 of 3.3%; for SAM these values are lower: 1.2 and 2.6%, respectively. The projections obtained for the SAM domain are lower than those obtained by Krüger et al. (2012) and Reboita et al. (2018) because here only more intense systems are considered. The values projected for the AUS domain are also lower than in previous work over southeast Australia, where Pepler et al. (2016) found a decrease of 16.7% in austral winter cyclones.

Figure 5 shows the frequency distribution of cyclone maximum depth (maximum value obtained during the whole lifecycle of each cyclone), lifetime and mean speed over the AFR, AUS and SAM domains in the ERAI, GCMs and RegCM4 ensembles, for the present and future climate. Overall, the models reproduce the distributions of cyclone characteristics found in ERAI, except in some instances such

as an underestimation of cyclone maximum depth over the Africa domain. The RegCM4 ensemble does not show a systematic improvement of cyclone statistics compared to the driving GCMs.

Concerning the climate change signals, the ensembles suggest in all domains a decrease of the frequency of low intensity (depth) cyclones and an increase in the frequency of high intensity ones (but without statistical significance at  $\alpha=0.05$ ; Fig. 5a–c), which is in agreement with previous studies (Grieger et al. 2014; Chang 2017; Kodama et al. 2019). In present climate, the cyclone lifetime has a strong peak at 24–48 h, with a sharp decrease for longer lasting cyclones (Fig. 5d–f). This pattern is not significantly changed in the future time slice. Similarly, the mean speed, which peaks in the range of 6–12 m s<sup>-1</sup> (Fig. 5g–i), and the traveled distance (figures not show) do not show strong variations in the future climate. Thus, overall Fig. 5 suggests that the characteristics of cyclones are not strongly modified by the projected global warming conditions.

From the differences between the RegCM4 and GCMs ensembles (Figs. 4, 5 and Table 2) it is noted that the RCM physics modifies the trend signal and/or intensity compared to the GCMs (e.g. Torma et al. 2015; Giorgi et al. 2016; Torma and Giorgi 2020). According to Torma et al. (2015) and Giorgi et al. (2016), the RCM downscaling has physically consistent fine-scale processes (for example, topographical forcing, land-cover etc.) and it does not simply represent a



**Fig. 5** Frequency polygon of the depth (hPa), lifetime (hour) and mean speed (m s<sup>-1</sup>) of the cyclones occurred in JJA in the GCMs and RegCM4 ensembles in the present (ENS-P; continuous line) and future climate (ENS-F; dashed line)

high-resolution disaggregation of the GCM fields to fine-scale, making possible different signal/intensity in RCMs and driving GCM.

### 3.2.3 Cyclogenesis hotspot regions and associated precipitation

We begin this section with a brief description of the trend in the total winter precipitation climatology under RCP8.5 over the three domains, in both RegCM4 and GCMs ensembles (more details about the validation of precipitation in the present-day and the climate change signal can be obtained in other papers of this special issue, such as Jacob et al. 2020).

Figures 6, 7, 8, 9, 10 show the precipitation associated with cyclones in the present and future climate, along with the regions where the total winter precipitation climatology (not only due to cyclones) increases in the future compared to the present (that are indicated by black lines in Figs. 6, 7, 8, 9, 10c, f). Considering total winter precipitation, for the AFR domain, there are positive trends of precipitation from the southern border of the continent to higher latitudes (Fig. 6c, f). A similar pattern occurs over the AUS domain (Fig. 7c, f), specifically from the southeastern border of the continent to New Zealand. Moreover, there is a positive trend over large part of the continent. Over the SAM domain

(Fig. 9c, f), we find an increase of precipitation at the end-of-century for the region extending from southeast South America to the southwestern South Atlantic Ocean, a result that is in agreement with Llopart et al. (2020). In summary, the projections indicate a positive tendency for precipitation over the preferential cyclonic regions, even though the cyclone frequency is projected to decrease (Fig. 4f, g). This implies a tendency for increased precipitation for individual cyclones.

We also analyzed the 3-day mean precipitation (in  $\text{mm day}^{-1}$ ) associated with coastal cyclogenetic hotspot regions. For the SAM and AUS domains, two hotspot regions were selected, while only one for AFR (Fig. 1). For each hotspot region, the dates of cyclogenesis were used to calculate the mean precipitation from the previous day (day - 1) to the day after (day + 1) the cyclogenesis. This procedure is similar to that from Reboita et al. (2012), but somehow different from Reboita et al. (2018) and Kodama et al. (2019), who considered only the precipitation in a radius of  $8^\circ$  and  $5^\circ$ , respectively, during the entire cyclone lifecycle (then much of the precipitation of the fronts associated with the cyclones is not computed). This can justify possible differences obtained in our analysis when compared to these authors.

The 3-day mean precipitation associated with cyclogenesis in the present climate was validated through a

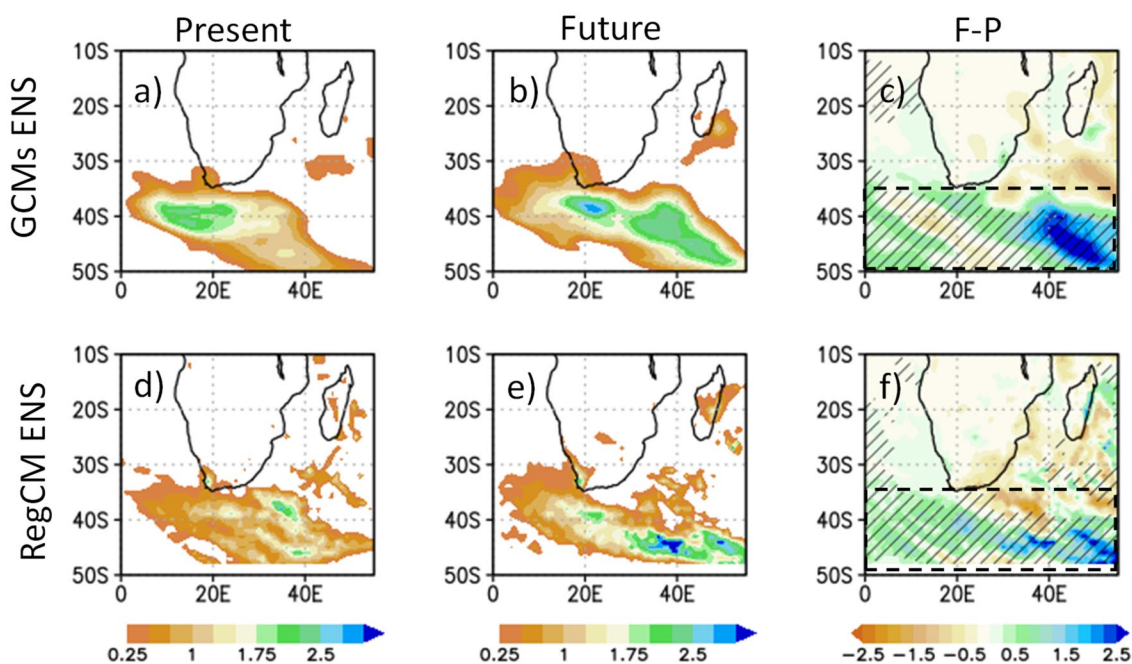


**Fig. 6** Precipitation associated with the cyclones in AFR hotspot region: **a, b, d** and **e** are the 3-day mean precipitation (from pre and post-cyclogenesis) minus the total winter climatology ( $\text{mm day}^{-1}$ ; only positive differences are shown) and **c, f** in colors, are the difference of the precipitation ( $\text{mm day}^{-1}$ ) associated with the cyclones (3-days) in the future minus the present (F-P) and in black lines the

places where the total winter precipitation climatology will increase in the future compared to the present. Top: GCMs ensemble and bottom: RegCM4 ensemble. In figures **c, f** the black dashed box represents the area used to calculate the mean of 3-day precipitation in Table 3

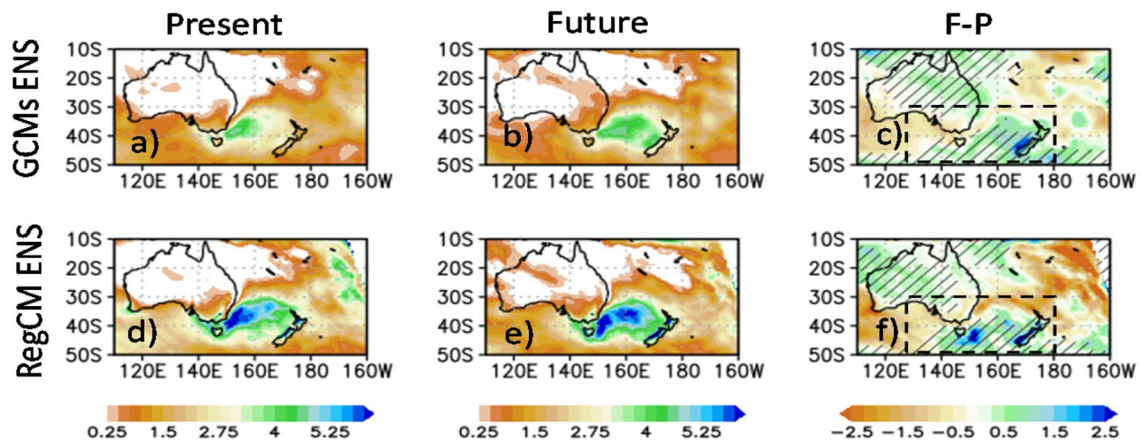


Fig. 7 Similar to Fig. 6, but for the precipitation associated with the cyclones in AUS1 hotspot region

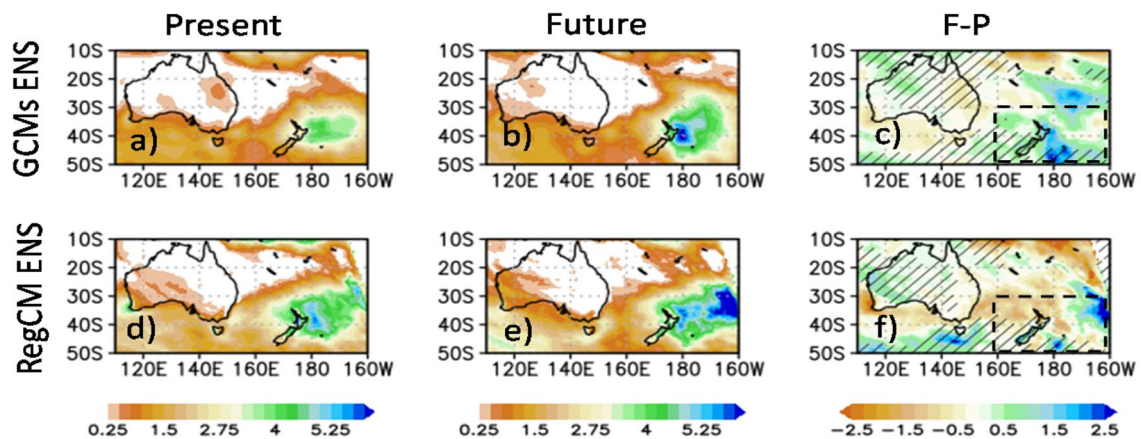


Fig. 8 Similar to Fig. 6, but for the precipitation associated with the cyclones in AUS2 hotspot region

comparison with GPCP observations (figures not shown), i.e., the precipitation registered in the cyclones identified in ERAI. The model ensembles underestimate the precipitation intensity ( $\text{mm day}^{-1}$ ) in the AFR, SAM1 and SAM2 regions compared to GPCP, while they overestimate precipitation in the AUS1 region. In AUS2 the simulated precipitation is close to the GPCP analysis.

Figures 6, 7, 8, 9, 10a, d shows the difference of the 3-day mean precipitation associated with cyclogenesis in the hotspot regions with respect to the total winter precipitation for the GCMs and RegCM4 ensembles in the present climate, while Figs. 6, 7, 8, 9, 10b, e show the same information for the future climate. The climate change signal of the 3-day mean precipitation (future minus present climate) is shown in colors in Figs. 6, 7, 8, 9, 10c, f. The intensity of precipitation is higher during the cyclogenetic events than for the winter total climatology (Figs. 6, 7, 8, 9, 10a, b, d, e). By comparing panels a–d (present) with b–e (future), it is noted that the RegCM4 and GCMs ensembles project

an increase of the cyclone precipitation intensity in relation to the winter climatology. Moreover, as in Kodama et al. (2019), the area of most intense precipitation increases in the future. These characteristics are consistent between the RegCM4 and GCMs ensembles. Considering the individual hotspot regions, in the AFR domain the increase of precipitation intensity occurs mainly near the southwestern coast of the continent; in AUS1 the increase occurs between southeastern Australia and New Zealand, mainly in RegCM4; in AUS2 it occurs over north New Zealand; and in SAM1 and SAM2 there is an expansion of the area with maximum precipitation intensity near southern Brazil/Uruguay and east of  $60^\circ \text{W}$  near  $40^\circ \text{S}$ , respectively.

In terms of the climate change signal (Figs. 6, 7, 8, 9, 10c, f), in all hotspot regions, we find a predominant increase in the mean intensity of the cyclogenetic precipitation in the future climate. For example, Fig. 9c, f shows more intense precipitation over southern Brazil and between Uruguay and Argentina with an increase greater than 30% in the future.

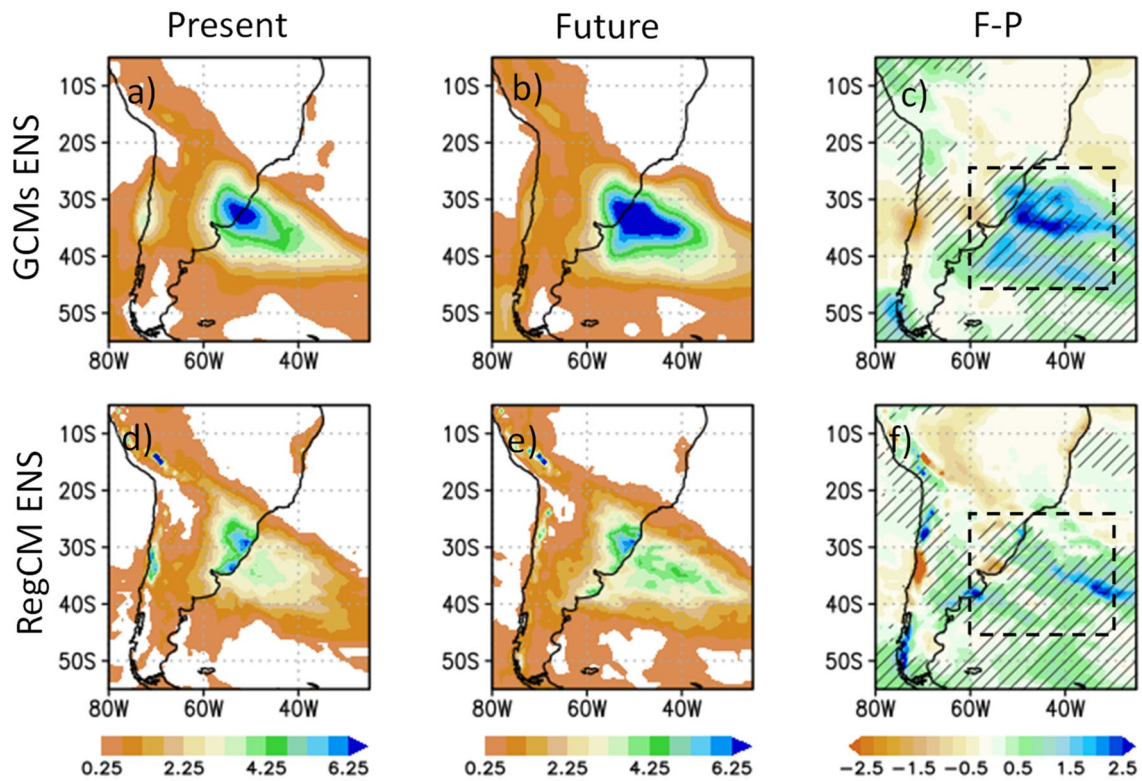


Fig. 9 Similar to Fig. 6, but for the precipitation associated with the cyclones in SAM1 hotspot region

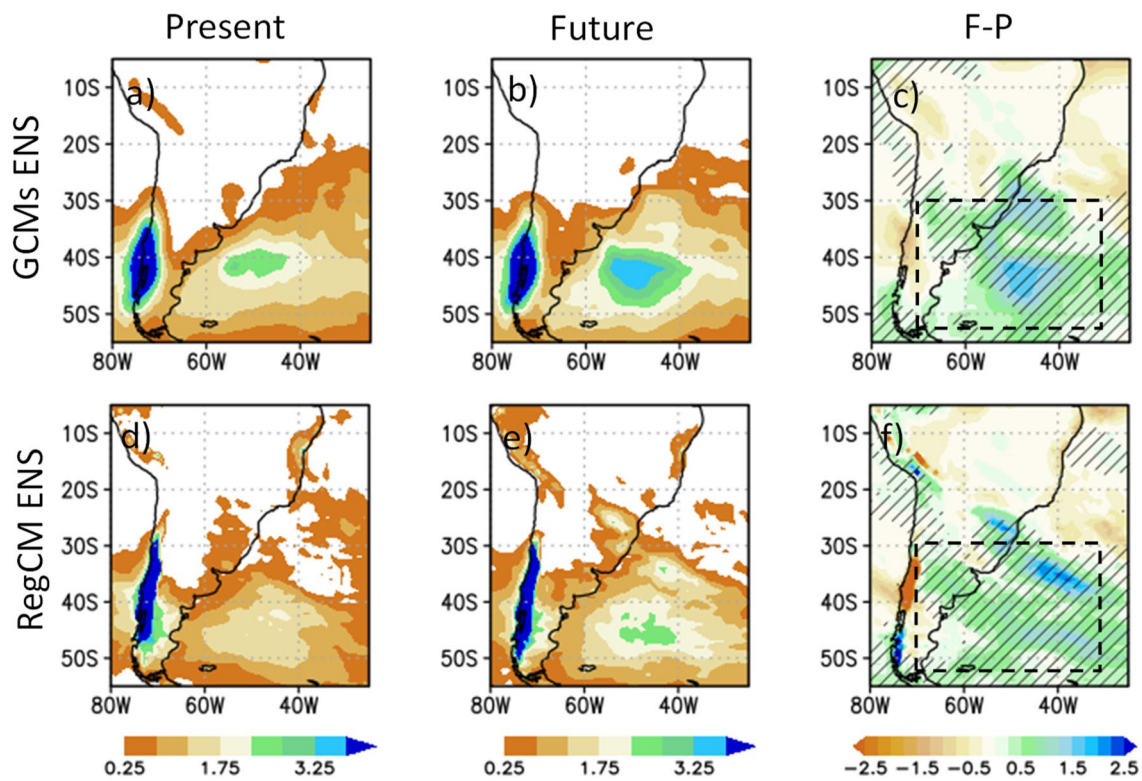


Fig. 10 Similar to Fig. 6, but for the precipitation associated with the cyclones in SAM2 hotspot region

Another way to evaluate the increase of precipitation amount associated with the cyclones in the future climate is by calculating the ratio between 3-day mean precipitation in the areas shown in Figs. 6, 7, 8, 9, 10 and the annual mean frequency of the cyclones of each hotspot region (Fig. 1). This provides a climatological value of the precipitation per cyclone (in mm day<sup>-1</sup>) in present and future climate. Table 3 shows that the rainfall amount associated with the individual cyclones will increase in the future, with the change in these ratios being statistically significant at the 95% confidence level according to Student t test.

The increase of precipitation intensity associated with cyclones is in agreement with Kodama et al. (2019) and with the literature compilation of Catto et al. (2019). These authors attribute the increase of the precipitation intensity to the increase of the latent heating and water holding capacity of the atmosphere in the climate change scenario, which is explained by the Clausius–Clapeyron relationship. In summary, our results indicate that the precipitation associated with individual storms will increase on average, i.e., that global warming will lead to a regime shift towards less frequent but more intense storms in terms of precipitation. This is consistent with the regime shifts found for example by Giorgi et al. (2011, 2019).

### 4 Conclusions

This study presents a comprehensive evaluation of the present and future (RCP8.5) cyclone climatology over the extratropical Southern Hemisphere during the winter using RegCM4 and GCMs ensembles completed as part of the CORDEX-CORE initiative (Gutowski et al. 2016). From CORDEX phase 1 to phase 2, the RegCM4 horizontal grid spacing changed from 50 to 25 km allowing a more realistic representation of the physical structure of the cyclones, which is one added value of the RegCM4.

The synoptic activity is analyzed over three domains (AFR, AUS and SAM) using the Eulerian and Lagrangian

approaches. Although the Eulerian analysis shows an increase of synoptic activity south of 40° S for the end-of-century time slice (2080–2099) compared to the present (1995–2014) in both the RegCM4 and GCMs ensembles, this signal does not necessarily indicate an increase in the cyclone frequency since it includes cyclonic and anticyclonic features. Indeed, the Lagrangian analysis, in which only the cyclones were tracked, shows a decrease in cyclone frequency in all domains considered. In this analysis, only cyclones with lifetime and depth equal or higher than 24 h and 10 hPa, respectively, are included (weaker cyclones are excluded).

The main results obtained from the Lagrangian approach are summarized as:

*Frequency:* except for the AFR domain, the decrease of cyclone frequency at the end of the century is statistically significant. For the AUS domain, the GCMs and RegCM4 ensembles project a decrease of 5.6% and 3.3%, respectively; in the SAM the negative trends are 1.2 and 2.6%, respectively;

*Intensity:* positive trends in the frequency of intense cyclones are found in the three domains. Although they are not statistically significant at the 95% confidence level, the trend signal is in agreement with Grieger et al. (2014), Chang (2017) and Kodama et al. 2019, and may explain the positive trend of precipitation projected under the RCP8.5 scenario;

*Lifetime, traveled distance and mean speed:* these cyclone features do not present statistically significant changes in the future climate compared to the present one;

*Precipitation:* the 3-day mean intensity of the precipitation associated with all cyclogenesis is projected to increase. In addition, the projections indicate an expansion of the area with more intense precipitation surrounding the hotspots cyclogenetic regions. Considering the cyclogenesis in the hotspot regions there is a statistically significant trend of each cyclone to produce more rainfall in the future climate.

Our results are generally in line with indications of a precipitation shift towards a regime of less frequent but more intense events in response to global warming, as found in previous studies (Giorgi et al. 2011, 2019). However, we also find a substantial regional dependence on these responses, which warrants further investigation with larger ensembles in order to provide more robust information for impact applications. Nevertheless, our findings do point to an increased hydroclimatic risk related not only to greater convection in warmer climates but also to extratropical cyclones. This increased risk is especially relevant

**Table 3** Precipitation rate (mm day<sup>-1</sup>) obtained as the ratio between the 3-days (from previous day to one day after cyclogenesis) mean precipitation in the areas shown in Figs. 6, 7, 8, 9, 10 and the annual mean of the cyclone frequency of each hotspot region

Hotspot regions	GCM-P	GCM-F	RegCM4-P	RegCM4-F
AFR	3.8	4.9	1.9	2.9
AUS1	1.6	2.3	3.2	3.5
AUS2	1.9	3.0	3.4	4.5
SAM1	2.7	3.1	2.3	2.5
SAM2	1.1	1.8	0.9	1.6

Differences between present (P) and future (F) climates are significant statistically ( $\alpha=0.05$ ) according to Student t-test

for coastal regions, which are particularly vulnerable to the effect of strong cyclonic activity.

**Acknowledgements** The authors thank CMIP5, ECMWF and GPCP for the data used in this study and ICTP and the National Council for Scientific and Technological Development (CNPq—Brazil) for financial support. M. Reale has been supported in this work by OGS and CINECA under HPC-TRES award number 2015-07 and by the project FAIRSEA (Fisheries in the Adriatic Region—a Shared Ecosystem. Approach) funded by the 2014–2020 Interreg V-A Italy—Croatia CBC Programme (Standard project ID 10046951). Special thanks for Talina Sines and Francesca Raffaele, who ran the projections from the domains used in this study.

## References

- Adeniyi MO (2019) Sensitivity of two dynamical cores in RegCM47 to the 2012 intense rainfall events over West Africa with focus on Lau, Nigeria. *Int J Model Simul* 1:1. <https://doi.org/10.1080/02286203.2019.1641777>
- Ashley WS, Black AW (2008) Fatalities Associated with Nonconvective High-Wind Events in the United States. *J Appl Meteorol Climatol* 47(2):717–725. <https://doi.org/10.1175/2007JAMC1689.1>
- Bader J, Mesquita MDS, Hodges KI, Keenlyside N, Osterhus S, Miles M (2011) A review on Northern Hemisphere sea-ice, storminess and the North Atlantic Oscillation: Observations and projected changes. *Atmos Res* 101(4):809–834. <https://doi.org/10.1016/j.atmosres.2011.04.007>
- Bentsen M, Bethke I, Debernard JB, Iversen T, Kirkevåg A, Seland O, Drange H, Roelandt C, Seierstad IA, Hoose C, Kristjansson JE (2012) The Norwegian Earth System Model, NorESM1-M—Part 1: Description and basic evaluation. *Geosci Model Dev Discuss* 5(3):2843–2931. <https://doi.org/10.5194/gmdd-5-2843-2012>
- Bengtsson L, Hodges KI, Keenlyside N (2009) Will extratropical storms intensify in a warmer climate? *J Clim* 22(9):2276–2301. <https://doi.org/10.1175/2008JCLI2678.1>
- Bengtsson L, Hodges KI, Roeckner E (2006) Storm tracks and climate change. *J Clim* 19(15):3518–3543. <https://doi.org/10.1175/JCLI3815.1>
- Bitencourt DP, Manoel G, Acevedo OC, Fuentes MV, Muza MN, Rodrigues ML, Leal-Quadro MF (2011) Relating winds along the Southern Brazilian coast to extratropical cyclones. *Meteorol Appl* 18(2):223–229. <https://doi.org/10.1002/met.232>
- Blackmon ML (1976) Climatological spectral study of the 500 mb geopotential height of the northern hemisphere. *J Atmos Sci* 33(8):1607–1623. [https://doi.org/10.1175/15200469\(1976\)033<1607:ACSSOT>2.0.CO;2](https://doi.org/10.1175/15200469(1976)033<1607:ACSSOT>2.0.CO;2)
- Blázquez J, Solman SA (2018) Relationship between projected changes in precipitation and fronts in the austral winter of the Southern Hemisphere from a suite of CMIP5 models. *Clim Dyn*. <https://doi.org/10.1007/s00382-018-4482-y>
- Booth JF, Naud CM, Del Genio AD (2013) Diagnosing warm frontal cloud formation in a GCM: A novel approach using conditional subsetting. *J Climate* 26:5827–5845. <https://doi.org/10.1175/JCLI-D-12-00637.1>
- Brasiliense CS, Dereczynski CP, Satyamurty P, Chou SC, da Silva Santos VR, Calado RN (2018) Synoptic analysis of an intense rainfall event in Paraíba do Sul river basin in southeast Brazil. *Meteorol Appl* 25(1):66–77. <https://doi.org/10.1002/met.1670>
- Catto JL, Ackerley D, Booth JF, Champion AJ, Colle BA, Pfahl S, Pinto JG, Quinting JF, Seiler C (2019) The future of midlatitude cyclones. *Curr Clim Chang Rep*. <https://doi.org/10.1007/s40641-019-00149-4>
- Catto JL, Madonna E, Joos H, Rudeva I, Simmonds I (2015) Global relationship between fronts and warm conveyor belts and the impact on extreme precipitation. *J Clim* 28(21):8411–8429. <https://doi.org/10.1175/JCLI-D-15-0171.1>
- Chang EKM, Ma C-G, Zheng C, Yau AMW (2016) Observed and projected decrease in Northern Hemisphere extratropical cyclone activity in summer and its impacts on maximum temperature. *Geophys Res Lett* 43(5):2200–2208. <https://doi.org/10.1002/2016GL068172>
- Chang EKM (2017) Projected significant increase in the number of extreme extratropical cyclones in the southern hemisphere. *J Clim* 30:4915–4935
- Collins WJ, Bellouin N, Doutriaux-Boucher M, Gedney N, Hinton T, Jones CD, Liddicoat S, Martin G, O'Connor F, Rae J, Senior C, Totterdell I, Woodward S, Reichler T, Kim J, Halloran P (2008) Evaluation of the HadGEM2 model. Hadley Centre Technical Note HCTN 74, Met Office Hadley Centre, Exeter, U.K., <https://www.metoffice.gov.uk/learning/library/publications/science/climate-science>
- da Rocha RP, Sugahara S, Da Silveira RB (2004) Sea waves generated by extratropical cyclones in the South Atlantic Ocean: Hindcast and validation against altimeter data. *Weather Forecast* 19(2):398–410. [https://doi.org/10.1175/1520-0434\(2004\)019<0398:SWGPEC>2.0.CO;2](https://doi.org/10.1175/1520-0434(2004)019<0398:SWGPEC>2.0.CO;2)
- Dee DP, Uppala SM, Simmons AJ, Berrisford P, Poli P, Kobayashi S, Andrae U, Balmaseda MA, Balsamo G, Bauer P, Bechtold P, Beljaars ACM, van de Berg L, Bidlot J, Bormann N, Delsol C, Dragani R, Fuentes M, Geer AJ, Haimberger L, Healy SB, Hersbach H, Hólm EV, Isaksen I, Kallberg P, Köhler M, Matricardi M, McNally AP, Monge-Sanz BM, Morcrette JJ, Park BK, Peubey C, Rosnay P, Tavalotto C, Thépaut JN, Vitart F (2011) The ERA-Interim reanalysis: configuration and performance of the data assimilation system. *Q J R Meteorol Soc* 137(656):553–597. <https://doi.org/10.1002/qj.828>
- Dowdy AJ, Mills GA, Timbal B, Wang Y (2013) Changes in the Risk of Extratropical Cyclones in Eastern Australia. *J Clim* 26(4):1403–1417. <https://doi.org/10.1175/JCLI-D-12-00192.1>
- Dowdy AJ, Pepler A, Di Luca A, Cavicchia L, Mills G, Evans JP, Louis S, McInnes K, Walsh K (2019) Review of Australian east coast low pressure systems and associated extremes. *Clim Dyn*. <https://doi.org/10.1007/s00382-019-04836-8>
- Elguindi N, Giorgi F, Turuncoglu UU (2014) Assessment of CMIP5 global model simulations over the sub-set of CORDEX domains used in the Phase I CREMA Experiment. *Clim Change* 125(1):7–21. <https://doi.org/10.1007/s10584-013-0935-9>
- Fasullo JT, Trenberth KE (2008) The Annual Cycle of the Energy Budget. Part II: Meridional Structures and Poleward Transports. *J Clim* 21(10):2313–2325. doi:10.1175/2007JCLI1936.1
- Feser F, Barcikowska M, Krueger O, Schenk F, Weisse R, Xia L (2015) Storminess over the North Atlantic and northwestern Europe: a review. *Q J R Meteorol Soc* 141(687):350–382. <https://doi.org/10.1002/qj.2364>
- Flaounas E, Kelemen FD, Wernli H, Gaetner MG, Reale M, Sanchez-Gomez E, Lionello P, Calmanti S, Podracanin Z, Somot S, Akhtar N, Romera R, Conte D (2018) Assessment of an ensemble of ocean–atmosphere coupled and uncoupled regional climate models to reproduce the climatology of Mediterranean cyclones. *Clim Dyn* 51:1023–1040
- Francis JA, Francis VSJ (2012) Evidence linking Arctic amplification to extreme weather. *Geophys Res Lett* 39:1–6. <https://doi.org/10.1029/2012GL051000>
- Gan MA, Rao VB (1991) Surface cyclogenesis over South America. *Mon Weather Rev* 119(5):1293–1302
- Geng Q, Sugi M (2003) Possible Change of Extratropical Cyclone Activity due to Enhanced Greenhouse Gases and Sulfate Aerosols—Study with a High-Resolution AGCM. *J*

- Clim 16(13):2262–2274. [https://doi.org/10.1175/1520-0442\(2003\)16<2262:PCOECA>2.0.CO;2](https://doi.org/10.1175/1520-0442(2003)16<2262:PCOECA>2.0.CO;2)
- Giorgetta MA, Jungclaus J, Reick CH, Legutke S, Bader J, Böttinger M, Brovkin V, Crueger T, Esch M, Fieg K, Glushak K, Gayler V, Haak H, Hollweg H, Ilyina T, Kinne S, Kornbluh L, Matei D, Mauritsen T, Mikolajewicz U, Mueller W, Notz D, Pithan F, Raddatz T, Rast S, Redler R, Roeckner E, Schmidt H, Schnur R, Segsneider J, Six K, Stockhause M, Timmreck C, Wegner J, Widmann H, Wieners K, Claussen M, Marotzke J, Stevens B (2013) Climate and carbon cycle changes from 1850 to 2100 in MPI-ESM simulations for the Coupled Model Intercomparison Project phase 5. *J Adv Model Earth Syst* 5(3):572–597
- Giorgi F, Coppola E, Solmon F, Mariotti L, Sylla MB, Bi X, Elguindi N, Diro GT, Nair V, Giuliani G, Turuncoglu UU, Cozzini S, Guttler I, Obrien TA, Tawfik AB, Shalaby A, Zakey AS, Steiner AL, Stordal F, Sloan LC, Brankovic C (2012) RegCM4: model description and preliminary tests over multiple CORDEX domains. *Clim Res* 52:7–29. <https://doi.org/10.3354/cr01018>
- Giorgi F, Im ES, Coppola E, Diffenbaugh NS, Gao XJ, Mariotti L, Shi Y (2011) Higher Hydroclimatic Intensity with Global Warming. *J Clim* 24:5309–5324
- Giorgi F, Jones C, Asrar GR (2009) Addressing climate information needs at the regional level: the CORDEX Framework. *World Meteorological Organization (WMO) Bull* 58(3):175
- Giorgi F, Torma C, Coppola E, Ban N, Schar C, Somot S (2016) Enhanced summer convective rainfall at Alpine high elevations in response to climate warming. *Nature Geosci* 9:584–589
- Giorgi F, Raffaele F, Coppola E (2019) The response of precipitation characteristics to global warming from climate projections. *Earth Syst Dynam* 10:73–89. <https://doi.org/10.5194/esd-10-73-2019>
- Gramscianinov CB, Hodges KI, Camargo R (2019) The properties and genesis environments of South Atlantic cyclones. *Clim Dyn*. doi:10.1007/s00382-019-04778-1
- Grieger J, Leckebusch GC, Donat MG, Schuster M, Ulbrich U (2014) Southern Hemisphere winter cyclone activity under recent and future climate conditions in multi-model AOGCM simulations. *Int J Climatol* 34(12):3400–3416. <https://doi.org/10.1002/joc.3917>
- Gutowski WJ Jr, Giorgi F, Timbal B, Frigon A, Jacob D, Kang H-S, Raghavan K, Lee B, Lennard C, Nikulin G, O'Rourke E, Rixen M, Solman S, Stephenson T, Tangang F (2016) WCRP coordinated regional downscaling experiment (CORDEX): a diagnostic MIP for CMIP6. *Geosci Model Dev* 9:4087–4095. <https://doi.org/10.5194/gmd-9-4087-2016>
- Hawcroft MK, Shaffrey LC, Hodges KI, Dacre HF (2012) How much Northern Hemisphere precipitation is associated with extratropical cyclones?. *Geophys Res, Lett*, p 39
- Hawcroft M, Walsh E, Hodges K, Zappa G. (2018) Significantly increased extreme precipitation expected in Europe and North America from extratropical cyclones. *Environ Res Lett*. 13(12)
- Holtzlag AAM, De Bruijn EIF, Pan H-L (1990) A high resolution air mass transformation model for short-range weather forecasting. *Mon Weather Rev* 118:1561–1575
- Holtzlag AAM, Boville BA (1993) Local versus nonlocal boundary-layer diffusion in a global climate model. *J Clim* 6:1825–1842
- Hoskins BJ, Hodges KI (2019) The Annual Cycle of Northern Hemisphere Storm Tracks. Part II: Regional Detail *J Clim* 32(6):1761–1775. <https://doi.org/10.1175/JCLI-D-17-0871.1>
- Hoskins BJ, Hodges KI (2005) A New Perspective on Southern Hemisphere Storm Tracks. *J Clim* 18(20):4108–4129
- Huffman GJ, Adler RF, Morrissey MM, Bolvin DT, Curtis S, Joyce R, McGavock B, Susskind J (2001) Global precipitation at one-degree daily resolution from multisatellite observations. *J Hydrometeorol* 2(1):36–50. [https://doi.org/10.1175/1525-7541\(2001\)002<0036:GPAODD>2.0.CO;2](https://doi.org/10.1175/1525-7541(2001)002<0036:GPAODD>2.0.CO;2)
- Huntingford C, Marsh T, Scaife A et al (2014) Potential influences on the United Kingdom's floods of winter 2013/14. *Nature Clim Change* 4:769–777
- IPCC (2013) In: Stocker TF, Qin D, Plattner G-K, Tignor M, Allen SK, Boschung J, Nauels A, Xia Y, Bex V, Midgley PM (Eds.) *Climate Change 2013: The Physical Science Basis. Contribution of Working Group I to the Fifth Assessment Report of the Intergovernmental Panel on Climate Change*. Cambridge and New York, NY: Cambridge University Press, p. 1535. doi: 10.1017/CBO9781107415324
- Jacob D, Teichmann C, Remedio AC, Buelow K, Remke T, Kriegsmann A, Lierhammer L, Rechid D, Sieck K, Buntemeyer L, Weber T, Hoffmann P, Langendijk G, Coppola E, Giorgi F, Ciarlo J, Raffaele F, Giuliani G, Xuejie G, Sines TR, Torres A, Das S, di Sante F, Pichelli E, Glazer R, Ashfaq M, Bukovsky M, Im ES. (2020) Assessing mean climate change signals in the global CORDEX-CORE ensemble. *Clim Dyn*, special issue.
- Ji F, Pepler AS, Browning S, Evans JP, Luca AD (2018) Trends and low frequency variability of east coast lows in the twentieth century. *J South Hemis Earth Syst Sci*. <https://doi.org/10.22499/3.6801.001>
- Kain JS, Fritsch JM (1990) A one-dimensional entraining/detraining plume model and its application in convective parameterization. *J Atmos Sci* 47(23):2784–2802. [https://doi.org/10.1175/1520-0469\(1990\)047<2784:AODEPM>2.0.CO;2](https://doi.org/10.1175/1520-0469(1990)047<2784:AODEPM>2.0.CO;2)
- Kiehl J, Hack J, Bonan G, Boville B, Breigleb B, Williamson D, Rasch P (1996) Description of the NCAR Community Climate Model (CCM3). National Center for Atmospheric Research Tech Note NCAR/TN-420+STR, NCAR, Boulder, CO
- Koné B, Diedhiou A, Touré NE, Sylla MB, Giorgi F, Anquetin S, Bamba A, Diawara A (2018) Koba AT (2018) Sensitivity study of the regional climate model RegCM4 to different convective schemes over West Africa. *Earth Syst Dyn* 9:1261–1278. <https://doi.org/10.5194/esd-9-1261-2018>
- Krüger LF, da Rocha RP, Reboita MS, Ambrizzi T (2012) RegCM3 nested in HadAM3 scenarios A2 and B2: Projected changes in extratropical cyclogenesis, temperature and precipitation over the South Atlantic Ocean. *Clim Change* 113(3–4):599–621. <https://doi.org/10.1007/s10584-011-0374-4>
- Kodama C, Iwasaki T (2009) Influence of the SST Rise on Baroclinic Instability Wave Activity under an Aquaplanet Condition. *J Atmos Sci* 66(8):2272–2287. <https://doi.org/10.1175/2009JAS2964.1>
- Kodama C, Stevens B, Mauritsen T, Seiki T, Satoh M (2019) A new perspective for future precipitation change from intense extratropical cyclones. *Geophys Res Lett*. <https://doi.org/10.1029/2019GL084001>
- Lionello P, Cogo S, Galati MB, Sanna A (2008) The Mediterranean surface wave climate inferred from future scenario simulations. *Glob Planet Change* 63(2–3):152–162. <https://doi.org/10.1016/j.gloplacha.2008.03.004>
- Lionello P, Dalan F, Elvini E (2002) Cyclones in the Mediterranean region: The present and the doubled CO2 climate scenarios. *Clim Res* 22(2):147–159. <https://doi.org/10.3354/cr022147>
- Lionello P, Giorgi F (2007) Winter precipitation and cyclones in the Mediterranean region: future climate scenarios in a regional simulation. *Adv Geosci* 12:153–158
- Lionello P, Trigo IF, Gil V, Liberato MLR, Nissen KM, Pinto JG, Raible CC, Reale M, Tanzarella A, Trigo RM, Ulbrich S, Ulbrich U (2016) Objective climatology of cyclones in the Mediterranean region: a consensus view among methods with different system identification and tracking criteria. *Tellus A: Dynamic Meteorology and Oceanography* 68:1. <https://doi.org/10.3402/tellusa.v68.29391>
- Lionello P, Conte D, Reale M (2019) The effect of cyclones crossing the Mediterranean region on sea level anomalies on the Mediterranean Sea coast. *Nat Hazards Earth Syst Sci* 19:1541–1564

- Llopart M, Reboita MS, da Rocha RP (2020) Assessment of multi-model climate projections of water resources over South America CORDEX domain. *Clim Dyn*. 55:99–116. <https://doi.org/10.1007/s00382-019-04990-z>
- Lu J, Cai M (2009) Seasonality of polar surface warming amplification in climate simulations. *Geophys Res Lett* 36(16):L16704. <https://doi.org/10.1029/2009GL040133>
- Mahlalela PT, Blamey RC, Reason CJC (2019) Mechanisms behind early winter rainfall variability in the southwestern Cape. *S Afr Clim Dyn* 53(1–2):21–39. <https://doi.org/10.1007/s00382-018-4571-y>
- Mbienda AJK, Tchawoua C, Vondou DA, Choumbou VP, Kenfack C, Sadem CK, Dey S (2016) Impact of anthropogenic aerosols on climate variability over Central Africa by using a regional climate model. *Int J Climatol* 37(1):249–267
- Michaelis AC, Willison J, Lackmann GM, Robinson WA (2017) Changes in winter North Atlantic extratropical cyclones in high-resolution regional pseudo-global warming simulations. *J Clim* 30(17):6905–6925. <https://doi.org/10.1175/JCLI-D-16-0697.1>
- Mizuta R, Matsueda M, Endo H, Yukimoto S (2011) Future change in extratropical cyclones associated with change in the upper troposphere. *J Clim* 24(24):6456–6470. <https://doi.org/10.1175/2011JCLI3969.1>
- Moss RH, Edmonds JA, Hibbard KA, Manning MR, Rose SK, van Vuuren DP, Carter TR, Emori S, Kainuma M, Kram T, Meehl GA, Mitchell GA, Mitchell JFB, Nakicenovic N, Riahi K, Smith SJ, Stouffer RJ, Thomson AM, Weyant JP, Wilbanks TJ (2010) The next generation of scenarios for climate change research and assessment. *Nature* 463:747–756. <https://doi.org/10.1038/nature08823>
- Murray RJ, Simmonds I (1991) A numerical scheme for tracking cyclone centres from digital data: Part I: development and operation of the scheme. *Aust Meteorol Mag* 39(3):167–180
- Neu U, Akperov MG, Bellenbaum N, Benestad R, Blender R, Caballero R, Coccozza A, Dacre HF, Feng Y, Fraedrich K, Grieger J, Gulev S, Hanley J, Hewson T, Inatsu M, Keay K, Kew SF, Kindem I, Leckebusch GC, Liberato MLR, Lionello P, Mokhov II, Pinto JG, Raible CC, Reale M, Rudeva I, Schuster M, Simmonds I, Sinclair M, Sprenger M, Tilinina ND, Trigo IF, Ulbrich S, Ulbrich U, Wang XL, Wernli H (2013) IMILAST: a community effort to intercompare extratropical cyclone detection and tracking algorithms. *Bull Am Meteorol Soc* 94(4):529–547. <https://doi.org/10.1175/BAMS-D-11-00154.1>
- Nissen KM, Leckebusch GC, Pinto JG, Renggli D, Ulbrich S, Ulbrich U (2010) Cyclones causing wind storms in the Mediterranean: characteristics, trends and links to large-scale patterns. *Nat Hazards Earth Syst Sci* 10:1379–1391. <https://doi.org/10.5194/nhess-10-1379-2010>
- Núñez M, Blázquez J (2014) Climate change in La Plata basin as seen by a high-resolution global model. *Atmos Clim Sci* 4:272–289
- Oleson KW, Lawrence DM, Bonan GB, Drewniak B, Huang M, Koven CD, Levis S, Li F, Riley WJ, Subin ZM, Swenson SC, Thornton PE, Bozbiyik A, Fisher R, Kluzek E, Lamarque J-F, Lawrence PJ, Leung LR, Lipscomb W, Muszala S, Ricciuto DM, Sacks W, Sun Y, Tang J, Yang Z-L (2013) Technical Description of version 4.5 of the Community Land Model (CLM), Tech. rep., National Center for Atmospheric Research. <https://doi.org/10.5065/D6RR1W7M>
- Ogwang BA, Chen H, Li X et al (2016) Evaluation of the capability of RegCM4.0 in simulating East African climate. *Theor Appl Climatol* 124:303–313. <https://doi.org/10.1007/s00704-015-1420-3>
- Pal JS, Giorgi F, Bi X, Elguindi N, Solmon F, Gao X, Rauscher SA, Francisco R, Zakey A, Winter J, Moetasim A, Syed FS, Bell JL, Diffenbaugh NS, Karmacharya J, Konaré A, Martinez D, da Rocha RP, Sloan LC, Steiner AL (2007) Regional climate modeling for the developing world: the ICTP RegCM3 and RegCNET. *Bull Am Meteorol Soc* 88:1395–1409
- Pal JS, Small E, Eltahir E (2000) Simulation of regional-scale water and energy budgets: representation of subgrid cloud and precipitation processes within RegCM. *J Geophys Res* 105:29579–29594
- Peixoto JP, Oort AH, Covey C, Taylor K (1992) Physics of climate. *Phys Today* 45(8):67–67. <https://doi.org/10.1063/1.2809772>
- Pepler AS, Di Luca A, Ji F, Alexander LV, Evans JP, Sherwood SC (2016) Projected changes in east Australian midlatitude cyclones during the 21st century. *Geophys Res Lett* 43(1):334–340. <https://doi.org/10.1002/2015GL067267>
- Pepler A, Dowdy A, Hope P (2018) A global climatology of surface anticyclones, their variability, associated drivers and long-term trends. *Clim Dyn*. <https://doi.org/10.1007/s00382-018-4451-5>
- Pezza AB, Rashid HA, Simmonds I (2012) Climate links and recent extremes in Antarctic sea ice, high-latitude cyclones, southern annular mode and ENSO. *Clim Dyn* 38:57–73
- Pitt M (2008) Learning Lessons from the 2007 Floods. Cabinet Office, London
- Pfahl S, Wernli H (2012) Quantifying the relevance of cyclones for precipitation extremes. *J Clim* 25:6770–6780
- Reale M, Lionello P (2013) Synoptic climatology of winter intense precipitation events along the Mediterranean coasts. *Nat Hazards Earth Syst Sci* 13(7):1707–1722. <https://doi.org/10.5194/nhess-13-1707-2013>
- Reale M, Liberato MLR, Lionello P, Pinto JG, Salon S, Ulbrich S (2019) A global climatology of explosive cyclones using a multi-tracking approach. *Tellus A: Dyn Meteorol Oceanogr* 71(1):1–19. <https://doi.org/10.1080/16000870.2019.1611340>
- Reboita MS, da Rocha RP, Ambrizzi T, Sugahara S (2010) South Atlantic Ocean cyclogenesis climatology simulated by regional climate model (RegCM3). *Clim Dyn* 35(7):1331–1347. <https://doi.org/10.1007/s00382-009-0668-7>
- Reboita MS, da Rocha RP, Ambrizzi T (2012) Dynamic and climatological features of cyclonic developments over southwestern South Atlantic Ocean. *Horizons Earth Sci Res* 6:135–160
- Reboita MS, da Rocha RP, Dias CG, Ynoue RY (2014) Climate projections for South America: RegCM3 driven by HadCM3 and ECHAM5. *Adv Meteorol*. Article ID 376738, 17
- Reboita MS, da Rocha RP, Ambrizzi T, Gouveia CD (2015) Trend and teleconnection patterns in the climatology of extratropical cyclones over the Southern Hemisphere. *Clim Dyn* 45(7–8):1929–1944. <https://doi.org/10.1007/s00382-014-2447-3>
- Reboita MS, da Rocha RP, de Souza MR, Llopart M (2018) Extratropical cyclones over the southwestern South Atlantic Ocean: HadGEM2-ES and RegCM4 projections. *Int J Climatol* 38(6):2866–2879. <https://doi.org/10.1002/joc.5468>
- Reboita MS, da Rocha RP, Oliveira DM (2019a) Key features and adverse weather of the named subtropical cyclones over the Southwestern South Atlantic. *Atmosphere* 10(1):6. <https://doi.org/10.3390/atmos10010006>
- Reboita MS, Ambrizzi T, Silva BA, Pinheiro RF, da Rocha RP (2019b) The South Atlantic subtropical anticyclone: present and future climate. *Front Earth Sci* 7:8. <https://doi.org/10.3389/feart.2019.00008>
- Reichler T (2009) Changes in the atmospheric circulation as indicator of climate change. *Clim Change*. <https://doi.org/10.1016/B978-0-444-53301-2.00007-5>
- Rivière G, Arbogast P, Lapeyre G, Maynard K (2012) A potential vorticity perspective on the motion of a mid-latitude winter storm. *Geophys Res Lett* 39:L12808. <https://doi.org/10.1029/2012GL052440>
- Shaw TA, Baldwin M, Barnes EA, Caballero R, Garfinkel CI, Hwang Y-T, Li C, O’Gorman PA, Rivière G, Ir S, Voigt A (2016) Storm track processes and the opposing influences of climate 785 change. *Nat Geosci* 9:656–664



- Seth A, Rojas M, Rauscher SA (2010) CMIP3 projected changes in the annual cycle of the South American Monsoon. *Clim Change* 98:331–357. <https://doi.org/10.1007/s10584-009-9736-6>
- Sinclair MR (1994) An objective cyclone climatology for the Southern Hemisphere. *Mon Weather Rev* 122(10):2239–2265. [https://doi.org/10.1175/1520-0493\(1994\)122<2239:AOCFT>2.0.CO;2](https://doi.org/10.1175/1520-0493(1994)122<2239:AOCFT>2.0.CO;2)
- Sines T, Coppola E, Giorgi F, Sitz L (2018a) South America CORDEX project using RegCM. Available in: <https://indico.ictp.it/event/8313/session/2/contribution/9/material/slides/0.pdf>
- Sines T, Coppola E, Giorgi F (2018b) North America and Australasia CORDEX projects using RegCM. Available in: <https://indico.ictp.it/event/8313/session/8/contribution/40/material/slides/0.pdf>
- Song R, Gao X, Zhang H, Moise A (2008) 20 km resolution regional climate model experiments over Australia: experimental design and simulations of current climate. *Aust Meteorol Mag* 57(3):175–193
- Taylor KE, Stouffer RJ, Meehl GA (2012) An overview of CMIP5 and the experiment design. *Bull Am Meteorol Soc* 93(4):485–498. <https://doi.org/10.1175/BAMS-D-11-00094.1>
- Tiedtke M (1989) A comprehensive mass flux scheme for cumulus parameterization in large-scale models. *Mon Weather Rev* 117(8):1779–1800. [https://doi.org/10.1175/1520-0493\(1989\)117<1779:ACMFSF>2.0.CO;2](https://doi.org/10.1175/1520-0493(1989)117<1779:ACMFSF>2.0.CO;2)
- Torma C, Giorgi F (2020) On the evidence of orographical modulation of regional fine scale precipitation change signals: The Carpathians. *Atmos Sci Lett* 2020:e967. <https://doi.org/10.1002/asl.967>
- Torma CS, Giorgi F, Coppola E (2015) Added value of regional climate modeling over areas characterized by complex terrain: precipitation over the Alps. *J Geophys Res Atmos* 120:3957–3972. <https://doi.org/10.1002/2014JD022781>
- Ulbrich U, Leckebusch GC, Pinto JG (2009) Extra-tropical cyclones in the present and future climate: a review. *Theor Appl Climatol* 96(1–2):117–131. <https://doi.org/10.1007/s00704-008-0083-8>
- Ulbrich U, Leckebusch GC, Grieger J, Schuster M, Akperov M, Bardin MY, Feng Y, Gulev S, Inatsu M, Keay K, Kew SF, Liberato MLR, Lionello P, Mokhov II, Neu U, Pinto JG, Raible CC, Reale M, Rudeva I, Simmonds I, Tilinina ND, Trigo IF, Ulbrich S, Wang XL, Wernli H, Team TIMILAST (2013) Are Greenhouse Gas Signals of Northern Hemisphere winter extra-tropical cyclone activity dependent on the identification and tracking algorithm? *Meteor Z* 22:61–68. <https://doi.org/10.1127/0941-2948/2013/0420>
- Vera CS, Vighiarolo PK, Berbery EH (2002) Cold season synoptic-scale waves over subtropical South America. *Mon Weather Rev* 130(3):684–699. [https://doi.org/10.1175/1520-0493\(2002\)130<0684:CSSSWO>2.0.CO;2](https://doi.org/10.1175/1520-0493(2002)130<0684:CSSSWO>2.0.CO;2)
- Yin JH (2005) A consistent poleward shift of the storm tracks in simulations of 21st century climate. *Geophys Res Lett* 32(18):1. <https://doi.org/10.1029/2005GL023684>
- Zappa G, Shaffrey LC, Hodges KI (2013) The Ability of CMIP5 Models to Simulate North Atlantic Extratropical Cyclones. *J Clim* 26(15):5379–5396. <https://doi.org/10.1175/JCLI-D-12-00501.1>
- Zeng X, Zhao M, Dickinson RE (1998) Intercomparison of bulk aerodynamic algorithms for the computation of sea surface fluxes using TOGA COARE and TAO data. *J Clim*. [https://doi.org/10.1175/1520-0442\(1998\)011<2628:IOBAAF>2.0.CO;2](https://doi.org/10.1175/1520-0442(1998)011<2628:IOBAAF>2.0.CO;2)

**Publisher's Note** Springer Nature remains neutral with regard to jurisdictional claims in published maps and institutional affiliations.